Acta Odontologica Scandinavica. 2014; 72: 597–606

informa
healthcare

ORIGINAL ARTICLE

Preparation and properties of calcium-silicate filled resins for dental restoration. Part I: chemical-physical characterization and apatite-forming ability

ANDREA CORRADO PROFETA

Department of Restorative Dentistry, Biomaterials Science, Biomimetics and Biophotonics (B3) Research Group, King's College London Dental Institute, Guy's Dental Hospital, London, UK

Abstract

Objective. The aim of this study was to measure dimensional changes due to hygroscopic expansion and the bioactivity of two experimental methacrylate-based dental adhesives either incorporating Bioglass® 45S5 (3-E&RA/BG) or MTA (3-E&RA/WMTA). ***Materials and methods.*** 3-E&RA/BG, 3-E&RA/WMTA and a control filler-free resin blend (3-E&RA) were formulated from commercially available monomers. Water sorption (WS) and solubility (SL) behaviour were evaluated by weighing material disks at noted intervals; the relationship between degree of hydration and the glass transition temperature (*T*g) was investigated by using differential scanning calorimetry (DSC). *In vitro* apatite-forming ability as a function of soaking time in phosphate-containing solutions was also determined. Kruskal-Wallis analysis of variance (ANOVA) was used to evaluate differences between groups for maximum WS, SL, net water uptake and the percentage change in *T*g values. Post-ANOVA pair-wise comparisons were conducted using Mann-Whitney-U tests. ***Results.*** 3-E&RA/BG and 3-E&RA/WMTA exhibited values of maximum WS and net water uptake that were significantly higher when compared to 3-E&RA. However, no statistically significant differences were observed in terms of SL between all the adhesives. The addition of the Bioglass® 45S5 and MTA to the 3-E&RA showed no reduction of the *T*g after 60 days of storage in deionized water. ATR Fourier Transform Infrared Spectroscopy (ATR-FTIR) of the filled resin disks soaked in DPBS for 60 days showed the presence of carbonate ions in different chemical phases. ***Conclusion.*** Dentine bonding agents comprising calcium-silicates are not inert materials in a simulated oral environment and apatite formation may occur in the intra-oral conditions. ***Clinical significance.*** A bioactive dental material which forms apatite on the surface would have several benefits including closure of gaps forming at the resin–dentine interface and potentially better bond strength over time (less degradation of bond).

Key Words: *light-curable dental resin, bioactive micro-fillers, water sorption, water solubility, glass transition temperature, ATR Fourier transform infrared spectroscopy*

Introduction

The clinical success of composite restorations is compromised by the incomplete infiltration of currently used resinous materials into the demineralized dentine that leaves unprotected collagen fibrils below and within the resultant hybrid layer [1]. In an attempt to improve the durability of resin–dentine interfaces, it was speculated that dentine bonding agents (DBAs) containing Bioglass® 45S5 (BG) as ion-releasing micro-filler could be considered a promising approach for a possible therapeutic/protective effect associated with the precipitation of mineral compounds (i.e. apatite) within the collagen matrix [2]. Likewise, light-curable resins containing calcium-silicate Portland Cements have been proposed to deliver calcium and hydroxyl ions (alkalinizing activity) into the surrounding fluids and elicit a positive response at the interface from the biological environment [3].

It is common knowledge that release of ions from fillers in dentine adhesives and restoratives depends on the rate of water sorption (WS) and the segmental mobility of the polymer chains within the copolymerized, highly cross-linked resin matrix [4]. Their ion-leaching potential thus relies on the hydrophilic

Correspondence: Andrea Corrado Profeta, BDS PhD, Department of Restorative Dentistry, Biomaterials Science, Biomimetics and Biophotonics (B3) Research Group, King's College London Dental Institute, Floor 17, Tower Wing, Guy's Dental Hospital, Great Maze Pond, London SE1 9RT, UK. Tel: +44 020 7188 1824. Fax: +44 020 7188 1823. E-mail: andrea.profeta@kcl.ac.uk

(Received 18 September 2013; accepted 19 December 2013)

ISSN 0001-6357 print/ISSN 1502-3850 online
DOI: 10.3109/00016357.2013.878808

nature of the resin phase to absorb water for the necessary ion movement [5].

An important property in polymeric materials science is the glass transition temperature (*T*g) of the cured matrix which indicates degree of cross-linking, physical state and final mechanical properties of synthetic organic materials used as plastics and resins. It has been suggested that water absorbed into the adhesive polymers would result in a reduction of the *T*g and a weakening of the polymer network [6–8]. The *T*g reached after the incorporation of fillers into the adhesive would also depend on the amount of filler particles contained in its composition [9].

However, because of the novelty of these adhesives, the influence of the amount of WS on their thermal properties is still unknown. As such, the relationship between *T*g and degree of hydration needs to be determined.

Recent studies selected vibrational spectroscopy to investigate and identify a large range of components associated with dental materials [10,11]. Attenuated Total Reflection Fourier Transform Infrared Spectroscopy (ATR-FTIR) is often used to evaluate the *in vitro* apatite-forming ability of bioactive materials as a function of soaking time in phosphate-containing solutions (Dulbecco's Phosphate Buffered Saline, DPBS) [12].

Thus, the objective of this study was to investigate the performance of two new light-curable methacrylate-based DBAs either incorporating BG or a refined Portland Cement Type I (Mineral Trioxide Aggregate, MTA) with particular emphasis on the WS and solubility (SL) behaviour of the cross-linked networks under a simulated wet oral environment. For each material, the *T*g was characterized by using differential scanning calorimetry (DSC) directly after curing and following 60 days of storage in deionized water. The *in vitro* apatite-forming ability was assessed by ATR-FTIR technique after soaking in DPBS for 60 days.

The null hypotheses to be tested in this study were: (i) there is no difference between DBAs with respect to WS, SL and water uptake; (ii) there is no effect of water uptake and micro-filler content on the thermal properties (*T*g) of the tested adhesives; and (iii) milled DBAs possess bioactivity with the ability to form hydroxycarbonate apatite (HCAp) after immersion in DPBS.

Materials and methods

Experimental micro-fillers and resin blends formulation

A comonomer blend was formulated from commercially available monomers [13] by using 28.75 wt% of hydrophilic 2-hydroxyethyl methacrylate (HEMA) and 40 wt% of cross-linking dimethacrylate 2, 2-bis [4(2-hydroxy-3-methacryloyloxy-propyloxy)-phenyl] propane (Bis-GMA). 30 wt% of 2,5-dimethacryloyloxyethyloxycarbonyl-1,4-benzenedicarboxylic acid (PMDM) was included to obtain a dental bonding system with chemical affinity to Calcium (Ca^{2+}) (Table I). To make the resins light-curable, 0.25 wt % camphorquinone (CQ) and 1.0 wt% 2-ethyldimethyl-4-aminobenzoate (EDAB) were also added.

The calcium/sodium phosphosilicate (BG: 46.1 SiO_2, 2.5 P_2O_5, 26.9 CaO and 24.4 Na_2O, in mol%) was prepared using a conventional melt-quench route. Briefly, a mixture of SiO_2, P_2O_5, CaO and Na_2O (Sigma-Aldrich, Gillingham, UK) was melted in a platinum crucible at 10°C/min up to 1100°C and maintained for 1 h. The temperature was then raised to 1450°C (10°C/min) and maintained for 30 min. Finally, the molten glass was quenched into water (~20°C) to prevent crystallization, dehydrated in absolute ethanol for 3 h, dried overnight in a furnace at 110°C, milled and sieved (<20 μm average particle).

Manufacturer's recommendations of mixing 1 g of powder with 0.35 mL of sterile water for 1 min on a glass slab by using a stainless steel spatula were applied to white ProRoot MTA (WMTA) [14]. This was allowed to set in an incubator at 37°C for 24 h, grinded in an agate ball mill as well as being sieved to obtain a 20–30 μm-sized, hydrated calcium-silicate.

Hybrid photopolymerizable adhesive agents were prepared by mixing with a spatula for 30 s on a glass plate each individual micro-filler (40 wt%) and the neat resin (60 wt%) [15] in order to form an homogeneous paste. A generic label for every experimental material has been proposed to refer to the main components (3-E&RA, 3-E&RA/BG, 3-E&RA/WMTA). This made the accounting easier, but it is non-presumptive about molecular formula and structure.

Specimen preparation

Each co-monomer mixture was directly dispensed drop-by-drop into a Teflon split ring mould (7 mm in diameter and 1 mm thick) in an ordinary laboratory environment at ~23°C, taking care to make the adhesive bubble-free. The Teflon mould was then sandwiched between two glass slides covered with Mylar sheets to exclude atmospheric oxygen and the complete assembly was clamped. The resin was light-cured for 20 s on each side using a quartz-tungsten-halogen light-curing unit (Optilux VLC, Demetron Research Co., Danbury, CT, USA). The light-curing unit had an exit-window diameter of 5 mm and was operated at 600 mW/cm^2. The output intensity of the curing unit was verified before testing with a halogen radiometer (Optilux Radiometer Model 100P/N - 10503; Demetron Research Co.). Standardization of the distance between the light source and the specimen was provided by the

Table I. Composition (wt%) of the experimental resin blends used in this study and chemical structures of their constituent monomers. To obtain dental bonding systems with chemical affinity to Calcium (Ca^{2+}), an acidic functional monomer (PMDM) was included [13]. A binary photoinitiator system CQ/EDAB made the neat resin light-curable.

	Groups		
Monomers used in the tested resin blends	3-E&RA*	3-E&RA/BG**	3-E&RA/WMTA**
40 wt%* *or* 23.5 wt%** Bis-GMA	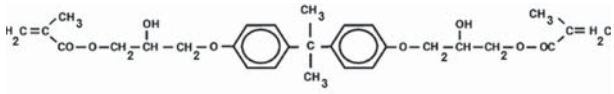		
28.75 wt%* *or* 17.25 wt% ** HEMA	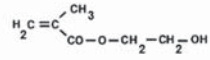		
30 wt%* *or* 18 wt%** PMDM	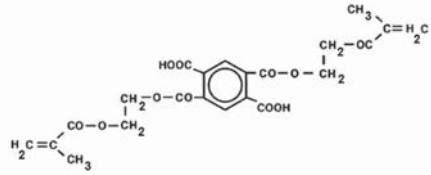		
Binary photoinitiator system		0.25 wt% CQ 1 wt% EDAB	
Micro-filler	No filler	40 wt% BG	40 wt% WMTA

Bis-GMA, 2,2-bis[4(2-hydroxy-3-methacryloyloxy-propyloxy)-phenyl] propane (Esstech, Essington, PA); HEMA, hydrophilic 2-hydroxyethyl methacrylate (Aldrich Chemical, Gillingham, UK); PMDM, 2,5-dimethacryloyloxyethyloxycarbonyl-1,4-benzenedicarboxylic acid (Esstech); CQ, camphoroquinone (Aldrich Chemical); EDAB, 2-ethyl-dimethyl-4-aminobenzoate (Aldrich Chemical); BG, Bioglass® 45S5 (SYLC, OSspray Ltd, London, UK); WMTA, white ProRoot MTA (Lot No. 08003395; Dentsply Tulsa Dental, Tulsa, OK).
*3-E&RA and means that the latter contains 40 wt% of Bis-GMA, 28.75 wt% of HEMA and 30 wt% of PMDM.
**3-E&RA/BG and 3-E&RA/WMTA meaning that these two groups contain 23.5 wt% of Bis-GMA, 17.25 wt% of HEMA and 18 wt% of PMDM.

thickness of the glass slide (1 mm), and the glass slides also provided a smooth surface for the testing process. Selection of curing time was determined in a pilot experiment by measuring a baseline microhardness of the surface of the resin disks (unpublished data). With the adopted total curing time (40 s), resins exhibited a mean Knoop microhardness of 20 ± 2 KHN that was sufficient to allow specimens to be removed from the Teflon mould without undergoing permanent deformation. Any specimen with visible voids was discarded. The excess material around the disks was removed using a scalpel blade and the margins were rounded and finished using 1000-grit silicon carbide grinding paper. The ultimate specimens (n = 10 per group) were flat and had very smooth surfaces. The thickness and diameter of the specimens were measured at four points using a digital caliper (Mitutoyo Corporation, Tokyo, Japan), rounded to the nearest 0.01 mm, and these measurements were used to calculate the volume (V) of each disk (in mm^3). The resin disks were then stored in a dessicator with silica gel at 37°C to ensure dryness for measurement of the initial mass. Each disk was weighed in an electronic analytical balance (Model AD6, PerkinElmer, Shelton, CT) with a reproducibility of ±0.1 mg until a constant mass (M0) was obtained (i.e. variation lower than 0.2 mg in 24 h), which was the baseline weight for the absorption–desorption cycle.

WS and SL evaluation

The protocol for this study was determined according to the ISO specification 4049 (2000) [16] except for the dimension of the specimen disks and the period of water storage that had been extended up to 60 days.

The specimens were individually immersed in Paraffin-sealed glass vials containing 20 ml of deionized water (pH 7.2) at 37 ± 0.5°C. At noted intervals (3, 5, 10, 24 h, 2, 3, 6, 9, 12, 15, 18, 21 days), each specimen was taken out of the glass vial using tweezers, blotted on a Whatman's filter paper to remove excess fluid, weighed and restored in fresh deionized water. The uptake of water was recorded until there was no significant change in weight, i.e. maximum wet mass of the surface-blotted water-equilibrated specimens (Ms) was attained.

The specimens then underwent desorption in a desiccator, as previously described, and weighed daily until a dried constant mass (MD) was obtained.

The values for WS and SL ($\mu g/mm^3$) were calculated for each specimen using the following equations [6]:
Because the mass variation of resin disks is the net result of both an increase in mass owing to water penetration and the decrease in mass owing to elution of low-molecular-weight monomers and of oligomers, the net water uptake was calculated as the sum of maximum WS and SL [17].

DSC investigation

The *T*g of the experimental bonding systems were characterized by the use of a Perkin-Elmer Jade DSC system (Perkin-Elmer Corp., Waltham, MA). The system was calibrated with zinc/indium.

Additional specimens ($n = 4$ per group) were produced under the same photoactivation conditions used in the WS kinetics experiments and divided into two groups. The *T*g values of the first groups were measured immediately after curing, and the *T*g values of the second groups were measured after 60 days. The second groups of specimens were stored in light-proof boxes after the curing procedure to prevent further exposure to light and in distilled water at 37 ± 0.5°C.

Two crimpled aluminium pans with perforations (diameter = 4 mm, 1.2 thick) were placed in the sample holder of the DSC furnace. Adhesive films (10–13 mg) were obtained from each specimen and these were sealed in one of two aluminum pans while the other pan was left empty as a reference. Each experimental adhesive was tested five times at a rate of 10°C/min under nitrogen gas (20 ml/min) over a two step heating/cooling cycle temperature range of −20 to 200°C, to eliminate any residual water. The analysis of DSC curves was carried out for the second heating run data in order to exclude the effect of any possible impurity, which might influence the thermal properties of the materials during the first heating cycle. The *T*g was determined by using the inflection mid-point of the initial S-shaped transition slope and determined from the onset with the aid of Perkin-Elmer Spectrum computer software. For each thermograph the *T*g was calculated three times and the average value was used as the result and for the purpose of comparison.

Statistics

Kruskal-Wallis analysis of variance (ANOVA) was used to evaluate whether there were any differences between groups for maximum WS, SL, net water uptake and the percentage change in *T*g values. The percentage change in *T*g values was used to compensate for some differences in initial *T*g values. Where a statistically significant *p*-value was observed ($p < 0.05$), post-ANOVA pair-wise comparisons were conducted using Mann-Whitney-U tests, with $p < 0.01$ regarded as statistically significant to compensate for multiple comparisons.

ATR-FTIR spectroscopy

Four disks ($n = 4$) were made per group according to the procedure previously described. *In vitro* bioactivity was determined by immersing the materials in a sealed cylindrical polystyrene holder (3 cm high and 4 cm in diameter) containing 5 mL of DPBS fluid. DPBS is a physiological-like buffered (pH 7.4) Ca- and Mg-free solution with the following composition (mM): K^+ (4.18), Na^+ (152.9), Cl^- (139.5), PO_4^{3-} (9.56, sum of $H_2PO_4^-$ 1.5 mM and HPO_4^{2-} 8.06 mM). The solution was replaced every 72 h. Infrared spectra were obtained immediately after curing and after 60 days of DPBS ageing at 37°C [18], using a Spectrum One FTIR spectrophotometer (Perkin-Elmer Corp., Norwalk, CT) equipped with a diamond crystal attenuated total reflection (ATR) accessory. Prior to the spectrophotometric analysis, each sample was rinsed with distilled water for 30 s to stop the exchange reactions and then completely air-dried. In addition, ATR/FTIR spectra were acquired from BG as well as MTA alone. The ATR area had a 2 mm diameter. The IR radiation penetration was ~2 μm. Spectra were collected in the range of 650–4000 cm^{-1} at 4 cm^{-1} resolution for a total of 88 scans for each spectrum and processed by smoothing, baseline correction and normalization with Spectrum One Software Version 5.0.1 (Perkin-Elmer Corp.). To avoid complications deriving from potential lack of homogeneity of the samples, five spectra were recorded on each specimen. The reported IR spectra were the average of the spectra recorded on five different points.

Results

WS and SL evaluation

All the specimens remained intact after the absorption and desorption cycles. No visible signs of discolouration, crazes or cracks were observed in the resin disks.

Table II shows a summary of mean (± SD) data for mass gain (maximum WS) and mass loss (SL). Since these processes occur simultaneously [19], they were added together to provide an estimate of the net water uptake.

Kruskal-Wallis analysis of variance indicated that maximum and net water uptake showed potential differences between groups ($p < 0.001$). Post-ANOVA contrasts indicated that all groups were different from each other.

Overall, the neat resin (3-E&RA) exhibited values of maximum WS, SL and net water uptake that were significantly lower when compared to its corresponding filled versions. With respect to WS, the 3-E&RA group absorbed the least amount of water, while 3-E&RA/BG showed the highest values (3-E&RA: 96.2 μg/mm^3 < 3-E&RA/WMTA: 215.5 μg/mm^3 < 3-E&RA/BG: 352.3 μg/mm^3) and all the DBAs differed statistically from each other ($p < 0.05$).

Following the same trend, the lowest value of net water uptake was observed for the comonomer blend with no filler (3-E&RA: 89.5 μg/mm^3 < 3-E&RA/WMTA: 218.9 μg/mm^3 < 3-E&RA/BG: 359 μg/

Table II. Summary of maximum water uptake (WS), solubility (SL) and net water uptake data.

Group	WS	SL	Net water uptake
3-E&RA	9.6%[a] 96.2 (± 7.3)	0.6%[a] −6.7 (± 5.1)	8.9%[a] 89.5 (± 12.5)
3-E&RA/BG	35.2%[b] 352.3 (± 3.4)	0.6%[a] 6.6 (± 2.4)	35.9%[b] 359 (± 1)
3-E&RA/WMTA	21.5%[c] 215.5 (± 10.7)	0.3%[a] 3.4 (± 5.5)	21.8%[c] 218.9 (± 5.2)

Values are mean (± standard deviation) in relative terms (1 μg/mm^3 = 0.001 mg/mm^3 × 100 = 0.1 mg/100 mm^3 = 0.1%) and in absolute terms (μg/mm^3) to provide comparisons to literature values which include both expressions.
For each parameter investigated, same superscript lower case letters (analysis in columns) indicate no statistically significant differences ($p > 0.05$).
Negative solubility values indicate that the dried constant mass obtained after final dessication (MD) was higher than the initial adhesive polymer mass before water immersion (M0), suggesting that the absorbed water may have not been completely eliminated.

mm^3), which was significantly different from the values obtained with the DBAs comprising calcium-silicates ($p < 0.05$).

The loss of dry mass following WS was defined as solubilization of resin (SL). No statistically significant differences between all the DBSs were observed for this parameter ($p > 0.05$).

DSC investigation

DSC thermograms displayed two heating/cooling cycles for each specimen during the heating programme. The upper part of the DSC curve represented the heating cycles, whereas the lower part represented the cooling cycles (Figure 1). The thermal heat-capacity changes of the *T*g obtained for the control and the two experimental DBAs during the second heating run are reported in Table III. This shows a summary of the mean data for initial *T*g, *T*g after ageing and the percentage change in *T*g.

For the 3-E&RA, the initial *T*g was 115.3°C, whereas initial *T*g values of 3-E&RA/BG and 3-E&RA/WMTA were 119.7°C and 117.2°C, respectively. After the ageing period, the *T*g for the 3-E&RA group increased to 121.3°C. The *T*g also increased at the end of the period of water storage for the two experimental DBAs, ranging between 131.2°C (3-E&RA/WMTA) and 140.7°C (3-E&RA/BG).

Table III. Mean and standard deviations for *T*g initially, after the ageing period and percentage change as determined by DSC analysis.

Group	*T*g/°C initial⋆	*T*g/°C aged⋆	Percentage change
3-E&RA	115.3 (0.4)	121.3 (3.5)	5.19 (3.12)[a]
3-E&RA/BG	119.7 (2.8)	140.7 (1.8)	17.64 (3.71)[b]
3-E&RA/WMTA	117.2 (6.1)	131.2 (4.9)	12.13 (5.07)[a,b]

Numbers in parentheses are standard deviations. Same letter indicates no differences in columns.
⋆Five measurements.

Kruskal-Wallis analysis of variance indicated that the percentage change in *T*g showed potential differences between groups ($p < 0.001$). Post-ANOVA contrasts indicated that the lowest percentage change in *T*g presented by the 3-E&RA group was not statistically different from the percentage change of the 3-E&RA/WMTA group and that the percentage change in *T*g for the 3-E&RA/BG group was not statistically different from the 3-E&RA/WMTA.

ATR-FTIR spectroscopy

The results of ATR-FTIR analyses are shown in Figure 2. Band assignments have been given according to the literature [20,21].

In the unmilled comonomer blend (3-E&RA), the group assignments of the IR absorption bands confirmed prominent bands at 1716, 1637, 1454 and 1162–1078 cm^{-1} attributed to the C=O, C=C, CH_2 and C-O-C vibrations (HEMA), respectively. Absorption bands at 1260, 1385, 1520–1610, 3000 and 3440 cm^{-1} were ascribed to C-O-C_6H_4,

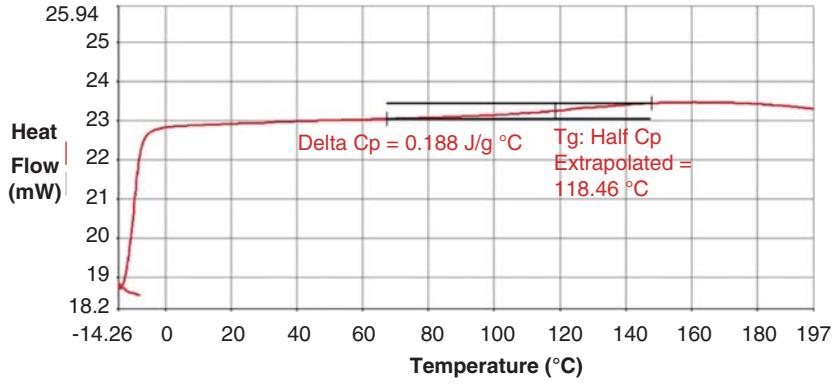

Figure 1. The glass transition temperature (*T*g) determined from the onset (*Tg*: Half Cp Extrapolated) of the heat capacity (Cp).

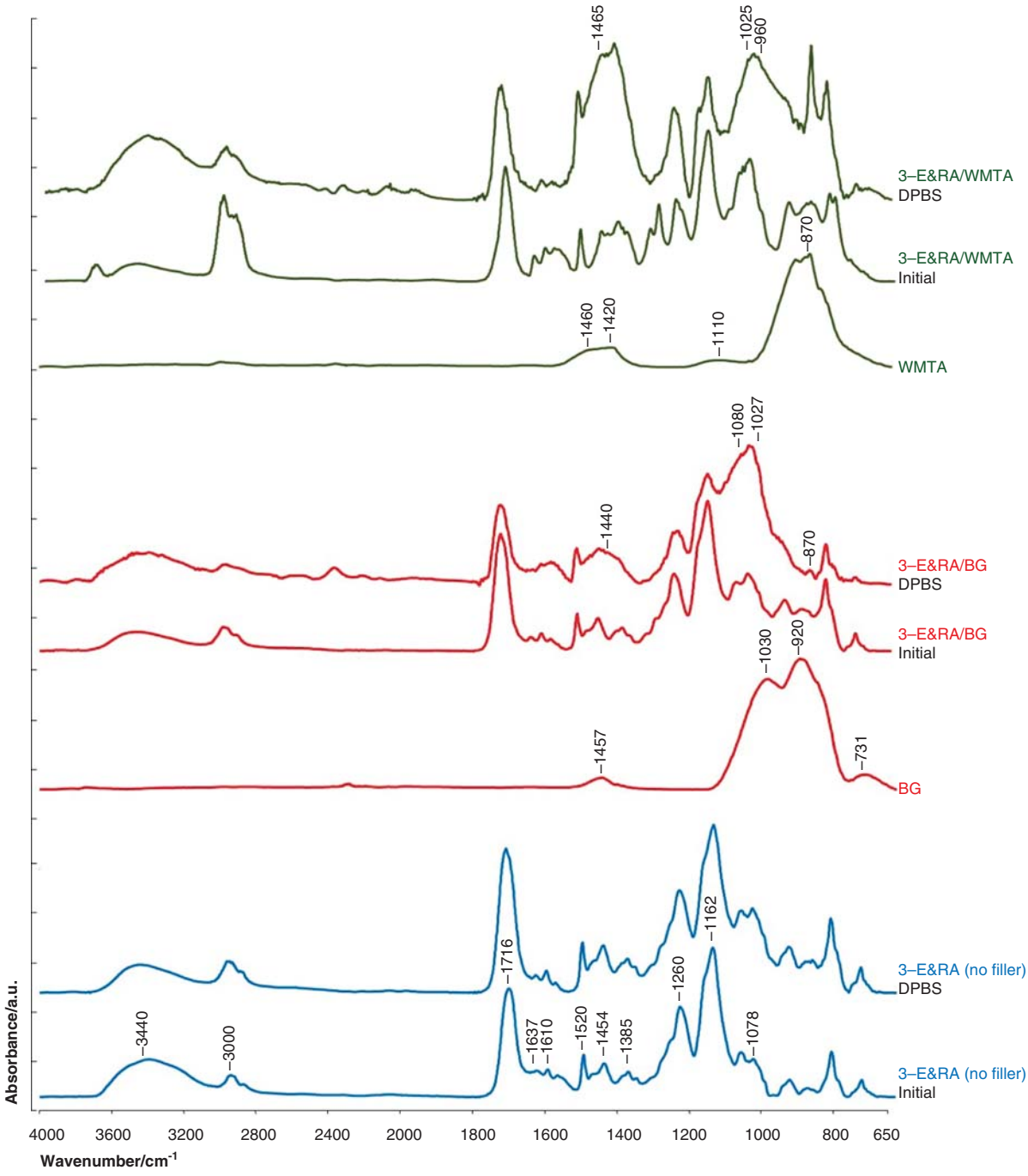

Figure 2. ATR-FTIR spectra of unmilled comonomer blends, micro-fillers and resin-based materials comprising calcium-silicates used in this study, immediately after curing and subsequent to 60 days of DPBS immersion.

CH_2, C_6H_4, C-H and OH vibrations (Bis-GMA), respectively.

The IR spectra of the hydrated calcium-silicate (WMTA) presented calcium carbonate bands at ~1460 cm^{-1} and 1420 cm^{-1}. The band at 1110 cm^{-1} can be associated with the SO_4^{2-} group. The 870 cm^{-1} band is attributable to belite.

IR spectra of the calcium sodium phosphosilicate powder (BG) were also obtained to characterize its chemical structure. BG powder presented vibrational bands at 731, 920, 1030 and 1457 cm^{-1}, corresponding to CO_3^{2-}, Si-O, Si-O-Si and CO_3^{2-} stretches, respectively [22].

Figure 2 also shows the FTIR-ATR spectra recorded on the outer surfaces of freshly prepared materials immediately after curing and of the samples soaked in DPBS for 60 days, revealing the presence of their respective constitutive elements.

With the exception of samples made of pure comonomer blend with 0 wt% micro-filler content

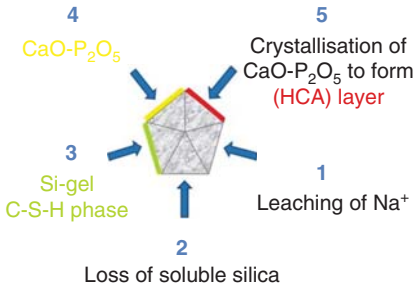

Figure 3. Schematic diagram of the bioactive micro-fillers reactions. In the presence of phosphate-containing solutions (DPBS), mineral crystals develop from dissolved precursor species on top of a silica nucleation layer. Calcium/sodium phosphosilicates (BG) and the silicate phases of Portland cements (WMTA) undergo a series of specific surface reactions with subsequent precipitation of an amorphous silica-rich layer 'Si-gel' or resulting in the formation of a nanoporous matrix/gel of calcium silicate hydrates 'C-S-H phase'. Subsequently, the formation of an over-saturated solution ($CaO\text{-}P_2O_5$), exceeding the solubility product constants for a number of mineral forms, induces hydroxycarbonate apatite (HCA) nucleation and crystal growth.

(3-E&RA), used as references to evaluate the structural evolution and the bioactivities of the prepared biomaterials, FTIR analyses proved the presence of HCAp on both the experimental adhesives after the ageing period.

The beginning of apatite deposition and a crystalline apatite phase were observed on the 3-E&RA/WMTA group, as primarily revealed by the higher resolution of the phosphate bending bands at 960, 1025 and 1465 cm^{-1}.

The bands present in the BG powder at 731 and 920 cm^{-1} disappeared in the corresponding 3-E&RA/BG adhesive after the soaking period, but a small carbonate (HCAp) band was present at 870 cm^{-1} [23]. The same spectra also showed a shoulder at 1080–1090 cm^{-1} due to the P-O stretch, and presence of orthophosphate at 60 days was confirmed by a clear-lypronounced orthophosphate band at 1027 cm^{-1}, superimposed on the Si-O-Si stretch band at 1030 cm^{-1}, which increased but did not markedly sharpen.

The absorption band at 1716 cm^{-1}, attributed to C=O stretching, can clearly be seen in the IR spectra of all the milled adhesives. This indicates that the C=O of the amide groups along the chains of HEMA was actively involved in the formation of the polymeric networks.

Discussion

The water absorption characteristics of any polymeric material, whether filled or not, is of great importance for dental applications. Ideally, polymer networks should be insoluble materials with relatively high chemical and thermal stability. Unfortunately, very few polymers are absolutely impermeable to water. Water is known to swell the resin polymer network and hydrolytically cleave methacrylate ester bonds [24]. This enables water percolation through the hybrid layer and may favour the rapid and catastrophic degradation of resin-dentine bonds [25].

However, some water absorption may not always be entirely disadvantageous [26] and this study explored the inclusion of two different ion-releasing fillers in an experimental dental adhesive as a way to benefit from the resin's hydrophilic behaviour and open up the potential to create favourably biointeractive dental adhesives. Hence, an evaluation of the water absorption characteristics of the polymeric biomaterials was clearly important.

By using the data obtained with the neat resin (3-E&RA) as a parameter for the relationship between WS and type of micro-filler, maximum water uptake and net water uptake were found to increase by adding BG or MTA to the polymer network, leading to partially reject the anticipated first null hypothesis and corroborating the results of previous studies [27].

After 60 days of storage in deionized water, all the experimental adhesives provided statistically significant increments relative to their initial *T*g that compelled the rejection of the second null hypothesis.

Conversely, the third null hypothesis was accepted, since ATR-FTIR analyses proved the presence of carbonated apatite on all the experimental adhesives after prolonged storage in DPBS.

In ISO 4049 [16], resin SL is calculated as a loss of dry mass in specimens that have been immersed in water over time. Unreacted monomers or oligomers can leach out of the polymer during WS and subsequent polymer expansion. Generally, increases in WS are associated with increases in SL. This is in contrast with the results of the present study in which no significant differences were observed for the latter between all the tested materials (Table II). A possible explanation for this controversy might be that the dried constant mass obtained after final dessication was higher than the initial adhesive polymer mass before water immersion, suggesting that the absorbed water may have not been completely eliminated and, thus, giving either poor (3-E&RA/BG and 3-E&RA/WMTA) or negative SL values (3-E&RA). However, this does not mean that no SL occurred, but rather that WS was greater than SL.

Since calcium and phosphate ion release is slow at later times [28], this could in part provide a further reason of the slight reduction in material mass and volume after 60 days.

Water diffuses into polymers at different rates depending on the polarity of their molecular structure, the degree of cross-linking and the presence of residual monomers and/or other water-attracting species, e.g. glass surfaces [29]. According to these molecular and microstructural factors, the mechanism of water diffusion can be summarized in two main theories: (i) free volume theory, according to

which water diffuses through nanometre spaces within the polymer; and (ii) interaction theory, according to which water binds to specific ionic groups of the polymer chain. In this case, water diffusion occurs according to water-affinity of these groups [30].

Water absorbed into resin polymers has been demonstrated to decrease the *T*g of dental adhesives. However, the damage is reversible at the outset with removal of the sorbed water [8].

After light-curing, the presence of Bis-GMA monomers in the experimental resin created a polymeric network able to stabilize the outer surface of the resin disks. Nonetheless, water-filled regions and/or hydrophilic polymer domains were also present in the cured resin [31], and these channels were thought to be responsible for water movement within the adhesives. Due to the hydrophilic pendant groups of HEMA, once immersed in aqueous medium the designed resin matrix was permeable enough to absorb water that was reused for hydrating the ionic products (PO_4^{3-} and Ca^{2+}) released from the water-soluble micro-fillers. This may explain why the addition of the bioactive particles to the control resin showed no reduction of the *T*g for the experimental adhesives.

As already pointed out in a previous work [32], *T*g variation has also been attributed to various molecular parameters, such as molecular weight and stiffness of the cross-linked chains. Along with a sustained and effective assimilation of water, the reactive fillers introduced phosphate and silicate groups that had a hindering effect on chain mobility; furthermore, secondary interactions were generated by the possible formation of oxygen bridges between close proximity phosphate and silicate groups within the copolymeric network, requiring a greater amount of energy to free the chains and, thus, raising the thermal heat-capacity of the material [33].

Intra-oral temperatures that exceed the *T*g may result in softening of the material and, consequently, in failure of the clinical procedure. It is equally important to observe that all the *T*g values obtained are well above the range of oral environment temperature.

The ability to release biologically active ions (biointeractivity) is a prerequisite for a material to be bioactive and trigger the formation of apatite. Hashimoto et al. [15] demonstrated that crystal formation was a common behaviour of adhesives prepared with 40 mass% bioglass and 60 mass% of light-cured resin containing Bis-GMA and HEMA during long-term water storage. The occurrence of similar chemical–physical events was recently reported in a light-curable MTA-based material containing an amphiphilic resin immersed in phosphate-containing solutions [12].

In this study, the ATR-FTIR spectroscopy technique yielded information on the chemical composition change which occurred on the surface of all the resin disks during the ageing period. As shown in Figure 1, IR spectra of 3-E&RA/WMTA resin disks soaked in DPBS for 60 days confirmed the presence of carbonate ions in different chemical phases, mainly as apatite deposits at 960, 1025 and 1465 cm^{-1}. In the 3-E&RA/BG adhesive, a small carbonate band at 870 cm^{-1} was taken as an indication for carbonate being incorporated into apatite, resulting in HCAp, rather than stoichiometric hydroxyapatite [34]. It was difficult to distinguish whether this band was split, in which case it would have been B-type substitution (i.e. carbonate replacing a phosphate group). However, broad CO_3^{2-} bands were present in the region starting from 1410–1440 cm^{-1}, indicating B-type substitution [35]. This was confirmed by the range of values (small shoulder-type peak) at 1080–1090 cm^{-1}, which are typically observed in B-type substituted HCAp [36].

It appears from the preceding discussion that the similarity in mode of biologic action of the micro-fillers employed in this study stems from one common characteristic they all possess: their propensity to release Ca^{2+} and the ability to form HCAp on the polymerized methacrylate.

It is important to consider that BG and the silicate phases of MTA when hydrated underwent a series of physicochemical reactions with subsequent precipitation of a polycondensated silica-rich layer 'Si-gel' (BG) [37] or resulting in the formation of a nanoporous matrix/gel of calcium silicate hydrates 'C-S-H phases' together with a soluble fraction of calcium hydroxide $Ca(OH)_2$ and portlandite (WMTA) [38]. Further incorporation of various mineral ions from the surrounding fluid helped the amorphous Si-gel and C-S-H phases to finally evolve into apatite crystals (Figure 3).

This process is governed mainly by a tailored surface charge; it has been previously demonstrated that negatively charged polar groups must be present for a catalytic effect on apatite nucleation [39]. Presumably, crystal formation also depends on the ion product being greater than the SL product constants of the solid phase formed on the material surface [40]. Indeed, the Si-gel and C-S-H phases provided the negatively charged sites for the migration of Ca^{2+} ions, which in turn led to an over-saturated solution that exceeded the SL product constants for a number of mineral forms, inducing crystal growth [41,42].

There is morphological evidence that the extent of permeability through the hybrid layer (nano-leakage) increases after 1 year of water storage [43,44], in consequence of the adsorption of water, hydrolysis of the ester bonds and component release processes in methacrylate materials [1].

As the crystallization process can bind water and encourage reprecipitation of less soluble species in material regions from which components have been released, it can also be anticipated that this might limit

nano-leakage and reduction in bond strength during long-term function.

Within the limitations of this study, it can be concluded that experimental methacrylate-based DBAs either incorporating BG or calcium-silicate cements are not inert materials in a simulated oral environment and the precipitation of apatite deposits in the surrounding fluid or contiguous dental tissues may occur in the intra-oral conditions.

A bioactive dental material which forms HCAp on the surface would have several benefits including closure of gaps forming at the resin–dentine interface and potentially better bond strength over time (less degradation of bond).

Future experiments will explore the functional consequences of WS values observed in this study on the micro-mechanical properties of the dentine adhesive interface. Ultra-morphology and micropermeability studies need to be performed when the same experimental adhesives are applied to acid-etched water-saturated dentine.

Acknowledgements

The author would like to thank Dr Ron Wilson of the Division of Periodontology, Dental Institute, King's College London for his expertise in statistical analysis.

***Declaration of interest*:** The author reports no conflicts of interest. The author alone is responsible for the content and writing of the paper.

References

[1] Spencer P, Ye Q, Park J, Topp EM, Misra A, Marangos O, et al. Adhesive/Dentin interface: the weak link in the composite restoration. Ann Biomed Eng 2010;38:1989–2003.

[2] Profeta AC, Mannocci F, Foxton RM, Thompson I, Watson TF, Sauro S. Bioactive effects of a calcium/sodium phosphosilicate on the resin-dentine interface: a microtensile bond strength, scanning electron microscopy, and confocal microscopy study. Eur J Oral Sci 2012;120: 353–62.

[3] Tay FR, Pashley DH. Biomimetic remineralization of resin-bonded acid-etched dentin. J Dent Res 2009;88:719–24.

[4] Ikemura K, Tay FR, Kouro Y, Endo T, Yoshiyama M, Miyai K, et al. Optimizing filler content in an adhesive system containing pre-reacted glass-ionomer fillers. Dent Mater 2003;19:137–46.

[5] Cattani-Lorente MA, Dupuis V, Moya F, Payan J, Meyer JM. Comparative study of the physical properties of a polyacid-modified composite resin and a resin-modified glass ionomer cement. Dent Mater 1999;15:21–32.

[6] Ito S, Hashimoto M, Wadgaonkar B, Svizero N, Carvalho RM, Yiu C, et al. Effects of resin hydrophilicity on water sorption and changes in modulus of elasticity. Biomaterials 2005;26:6449–59.

[7] Tay FR, Pashley DH, Suh BI, Carvalho RM, Itthagarun A. Single-step adhesives are permeable membranes. J Dent 2002; 30:371–82.

[8] Dhanpal P, Yiu CK, King NM, Tay FR, Hiraishi N. Effect of temperature on water sorption and solubility of dental adhesive resins. J Dent 2009;37:122–32.

[9] Sostena MM, Nogueira RA, Grandini CR, Moraes JC. Glass transition and degree of conversion of a light-cured orthodontic composite. J Appl Oral Sci 2009;17:570–3.

[10] Wang Z, Jiang T, Sauro S, Wang Y, Xing W, Liang S, et al. Nerve-targeted desensitizing toothpastes occlude dentin tubules and induce mineral precipitation. Am J Dent 2012;25:26–30.

[11] Kim YK, Gu LS, Bryan TE, Kim JR, Chen L, Liu Y. Mineralization of reconstituted collagen using polyvinylphosphonic acid/polyacrylic acid templating matrix protein analogues in the presence of calcium, phosphate and hydroxyl ions. Biomaterials 2010;31:6618–27.

[12] Gandolfi MG, Taddei P, Siboni F, Modena E, Ciapetti G, Prati C. Development of the foremost light-curable calcium-silicate MTA cement as root-end in oral surgery. Chemical-physical properties, bioactivity and biological behavior. Dent Mater 2011;27:e134–57.

[13] Code JE, Antonucci JM, Bennett PS, Schumacher GE. Photoactivated dentin bonding with N-phenyliminodiacetic acid. Dent Mater 1997;13:252–7.

[14] Dentsply TD. Directions for use ProRoot MTA (mineral trioxide aggregate) root canal repair material. Tulsa, OK: Dentsply Tulsa Dental. 2002.

[15] Hashimoto M, Iijima M, Nagano F, Ohno H, Endo K. Effect of monomer composition on crystal growth by resin containing bioglass. J Biomed Mater Res B Appl Biomater 2010;94: 127–33.

[16] ISO standard. ISO standard 4049: 2000 (E). Dentistry-polymer-based filling, restorative and luting materials. Geneva: ISO; 2000. p 18–21.

[17] Unemori M, Matsuya Y, Matsuya S, Akashi A, Akamine A. Water absorption of poly(methyl methacrylate) containing 4-methacryloxyethyl trimellitic anhydride. Biomaterials 2003; 24:1381–7.

[18] Gandolfi MG, Taddei P, Tinti A, Dorigo De Stefano E, Rossi PL, Prati C. Kinetics of apatite formation on a calcium-silicate cement for root-end filling during ageing in physiological-like phosphate solutions. Clin Oral Investig 2010;14:659–68.

[19] Tay FR, Pashley DH. Water-treeing - a potential mechanism for degradation of dentine adhesives. Am J Dent 2003;16: 6–12.

[20] Rueggeberg FA, Hashinger DT, Fairhurst CW. Calibration of FTIR conversion analysis of contemporary dental resin composites. Dent Mater 1990;6:241–9.

[21] Wang Z, Jiang T, Sauro S, Wang Y, Thompson I, Watson TF, et al. Dentine remineralization induced by two bioactive glasses developed for air abrasion purposes. J Dent 2011;39:746–56.

[22] Kim CY, Clark AE, Hench LL. Early stages of calcium-phosphate layer formation in bioglasses. J Non-Cryst Solids 1989;113:195–202.

[23] Lusvardi G, Malavasi G, Menabue L, Aina V, Morterra C. Fluoride-containing bioactive glasses: surface reactivity in simulated body fluids solutions. Acta Biomater 2009;5: 3548–62.

[24] Salz U, Zimmermann J, Zeuner F, Moszner N. Hydrolytic stability of self-etching adhesive systems. J Adhes Dent 2005; 7:107–16.

[25] Pashley DH, Tay FR, Yiu C, Hashimoto M, Breschi L, Carvalho RM, et al. Collagen degradation by host-derived enzymes during aging. J Dent Res 2004;83:216–21.

[26] Wei YJ, Silikas N, Zhang ZT, Watts DC. Hygroscopic dimensional changes of self-adhering and new resin-matrix composites during water sorption/desorption cycles. Dent Mater 2011;27:259–66.

[27] Yiu CK, King NM, Pashley DH, Suh BI, Carvalho RM, Carrilho MR, et al. Effect of resin hydrophilicity and water storage on resin strength. Biomaterials 2004;25:5789–96.
[28] Abou Neel EA, Palmer G, Knowles JC, Salih V, Young AM. Chemical, modulus and cell attachment studies of reactive calcium phosphate filler-containing fast photo-curing, surface-degrading, polymeric bone adhesives. Acta Biomater 2010;6:2695–703.
[29] Fabre HS, Fabre S, Cefaly DF, de Oliveira Carrilho MR, Garcia FC, Wang L. Water sorption and solubility of dentin bonding agents light-cured with different light sources. J Dent 2007;35:253–8.
[30] Malacarne J, Carvalho RM, De Goes MF, Svizero N, Pashley DH, Tay FR, et al. Water sorption/solubility of dental adhesive resins. Dent Mater 2006;22:973–80.
[31] Tay FR, Pashley DH, Yoshiyama M. Two modes of nanoleakage expression in single-step adhesives. J Dent Res 2002; 81:472–6.
[32] Min BG, Stachurski ZH, Hodgkin JH. Cure kinetics of elementary reactions of a DGEBA/DDS epoxy resin: 1. Glass transition temperature versus conversion. Polymer (Guildf) 1993;34:4908–12.
[33] Kemal E, Adesanya KO, Deb S. Phosphate based 2-hydroxyethyl methacrylate hydrogels for biomedical applications. J Mater Chem 2011;21:2237–45.
[34] Lu X, Leng Y. Theoretical analysis of calcium phosphate precipitation in simulated body fluid. Biomaterials 2005;26: 1097–108.
[35] Brauer DS, Karpukhina N, O'Donnell MD, Law RV, Hill RG. Fluoride-containing bioactive glasses: effect of glass design and structure on degradation, pH and apatite formation in simulated body fluid. Acta Biomater 2010;6:3275–82.
[36] LeGeros RZ, Trautz OR, Klein E, Legeros JP. 2 Types of carbonate substitution in apatite structure. Experientia 1969; 25:5–7.
[37] Andersson O, Kangasniemi I. Calcium phosphate formation at the surface of bioactive glass in vitro. J Biomed Mater Res A 1991;25:1019–30.
[38] Camilleri J. Characterization of hydration products of mineral trioxide aggregate. Int Endod J 2008;41:408–17.
[39] Welch K, Cai Y, Engqvist H, Strømme M. Dental adhesives with bioactive and on-demand bactericidal properties. Dent Mater 2010;26:491–9.
[40] Filgueiras MR, LaTorre GP, Hench LL. Solution effects on the surface reactions of a bioactive glass. J Biomed Mater Res 1993;27:445–53.
[41] Kokubo N, Kim HM, Kawashima M. Novel bioactive materials with different mechanical properties. Biomaterials 2003; 24:2161–75.
[42] Kim HM, Himeno T, Kokubo T, Nakamura T. Process and kinetics of bonelike apatite formation on sintered hydroxyapatite in a simulated body fluid. Biomaterials 2005;26: 4366–73.
[43] Tay FR, Hashimoto M, Pashley DH, Peters MC, Lai SCN, Yiu CKY, et al. Aging affects two modes of nanoleakage expression in bonded dentin. J Dent Res 2003;82:537–41.
[44] Hashimoto M, Ohno H, Sano H, Tay FR, Kaga M, Kudou Y, et al. Micromorphological changes in resindentin bonds after 1 year of water storage. J Biomed Mater Res 2002; 63:306–11.